JACS
JOURNAL OF THE AMERICAN CHEMICAL SOCIETY

Article

pubs.acs.org/JACS

From Ring-in-Ring to Sphere-in-Sphere: Self-Assembly of Discrete 2D and 3D Architectures with Increasing Stability

Bin Sun,[†,‡,▽] Ming Wang,[‡,▽] Zhichao Lou,[§,#] Mingjun Huang,[∥] Chenglong Xu,[⊥] Xiaohong Li,[⊥] Li-Jun Chen,[†] Yihua Yu,[†] Grant L. Davis,[‡] Bingqian Xu,*[,§] Hai-Bo Yang,*[,†] and Xiaopeng Li*[,‡]

[†]Shanghai Key Laboratory of Green Chemistry and Chemical Processes, Department of Chemistry, East China Normal University, Shanghai 200062, China

[‡]Department of Chemistry and Biochemistry, Texas State University, San Marcos, Texas 78666, United States

[§]Single Molecule Study Laboratory, College of Engineering and Nanoscale Science and Engineering Center, University of Georgia, Athens, Georgia 30602, United States

[∥]Department of Polymer Science, College of Polymer Science and Polymer Engineering, The University of Akron, Akron, Ohio 44325, United States

[⊥]College of Chemistry, Chemical Engineering and Materials Science, Soochow University, Suzhou 215123, China

[#]College of Materials Science and Technology, Nanjing University of Aeronautics and Astronautics, Nanjing 210016, China

Supporting Information

ABSTRACT: Directed by increasing the density of coordination sites (DOCS) to increase the stability of assemblies, discrete 2D ring-in-rings and 3D sphere-in-sphere were designed and self-assembled by one tetratopic pyridyl-based ligand with 180° diplatinum(II) acceptors and naked Pd(II), respectively. The high DOCS resulted by multitopic ligand provided more geometric constraints to form discrete structures with high stability. Compared to reported supramolecular hexagons and polyhedra by ditotpic ligands, the self-assembly of such giant architectures using multitopic ligands with all rigid backbone emphasized the structural integrity with precise preorganization of entire architecture, and required elaborate synthetic operations for ligand preparation. In-depth structural characterization was conducted to support desired structures, including multinuclear NMR (^{1}H, ^{31}P, and ^{13}C) analysis, 2D NMR spectroscopy (COSY and NOESY), diffusion-ordered NMR spectroscopy (DOSY), multidimensional mass spectrometry, TEM and AFM. Furthermore, a quantitative definition of DOCS was proposed to compare 2D and 3D structures and correlate the DOCS and stability of assemblies in a quantitative manner. Finally, ring-in-rings in DMSO or DMF could undergo hierarchical self-assembly into the ordered nanostructures and generated translucent supramolecular metallogels.

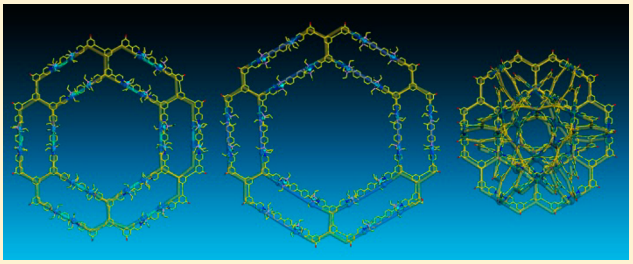

INTRODUCTION

Inspired by many functional biological systems created by nature, great efforts have been dedicated to the construction of novel supramolecular structures by exploiting a variety of noncovalent interactions, such as van der Waals, $\pi-\pi$ stacking, metal−ligand interactions, dipole−dipole interaction, hydrogen bonding, *etc.*[1] Benefiting from their versatile topological structures in a precisely controlled fashion at a wide range of length scales, these defect-free assemblies possess fascinating catalytic, electrochemical, photophysical, and magnetic properties with promising applications in energy, environmental, and biomedical fields.[2] Because of its highly directional and predictable feature, coordination-driven self-assembly has evolved into a well-established methodology for constructing novel two-dimensional (2D) and three-dimensional (3D) architectures based on specific stoichiometry, the geometry information instilled in the components, and the reaction conditions.[3−13] For instance, Stang et al. emphasized the angles of building blocks and summarized the general design principle for macrocycles using ditopic subunits.[2c,3l] Typically, under this design principle, using the combination of right-angular metal components and organic ligands should give rise to the predicted self-assembly macrocycles.

Guided by this principle, 2D metallo-supramolecular structures were mainly assembled by ditopic ligands and have matured in the context of a large variety of macrocycles.[14] However, multivalent interactions, which are extensively employed by nature to form stable secondary, tertiary, and quaternary structure of proteins, have not been as varied and significant as in biological systems. It is attributable to the challenge of design and synthesis of rigid multitopic ligands with precisely preorganized geometries for multivalent interactions. We reason that if multitopic ligands are designed

Received: November 6, 2014
Published: January 9, 2015

DOI: 10.1021/ja511443p
J. Am. Chem. Soc. 2015, 137, 1556−1564

with appropriate geometry, i.e., angles and distances, the self-assembly may lead to the construction of more sophisticated 2D architectures with desired shapes, sizes and increasing complexity, and thus to achieve optimal functionality. Furthermore, multitopic ligands assisted self-assembly may increase the coordination sites within a finite geometry, or density of coordination sites (DOCS),[15] and thus could increase the stability of 2D assemblies and facilitate characterization compared to conventional macrocycles. Nevertheless, self-assembly of large discrete 2D structures is more challenging than 3D structures from a standpoint of increasing the number of coordination and stability, because the orientation and interaction of 2D ligand is limited in plane geometry.

Directed by multitopic ligands assisted self-assembly, discrete hexagon wreaths with increasing complexity were obtained in our initial efforts through self-assembly of multitopic 2,2′:6′,2″-terpyridine ligands with Zn(II).[15] The success of using multitopic terpyridine ligand for the self-assembly of hexagon wreaths is reminiscent of pyridyl-based self-assembly, wherein both end-capped metal components and naked metal ions can be used to assemble a wide array of 2D and 3D structures.[4,5,10,11] Thus, multitopic pyridine ligands are able to serve as a more versatile platform to achieve more sophisticated supramolecular structures with increasing complexity than terpyridine-based ligands,[16] which are limited by the fixed 180° angle of ⟨terpyridine−metal(II)−terpyridine⟩ connectivity and centered on 2D self-assembly.[17]

To strengthen the design and self-assembly using multitopic ligands, we herein report the self-assembly of giant 2D ring-in-rings and 3D sphere-in-sphere using one tetratopic pyridyl-based ligand with end-capped Pt(II) components and naked Pd(II), respectively (Scheme 1). Compared to reported hexagons and polyhedra by ditotpic ligands,[2c,3o] the self-assembly using multitopic ligands requires more integrated design, elaborate synthetic operations and extensive characterization. With a careful control over directional bonding, higher DOCS can be realized within such complex structures. Note that we designed and evaluated a large pool of tetratopic ligand candidates with different geometry and linkers. According to molecular modeling, the structure of ligand **1** is the optimal one to generate desired structures with minimum geometric constraints as shown in Scheme 1. Therefore, using multitopic ligand with encoded geometry information, we are able to move beyond polygons and polyhedra to more complex structures with increasing numbers of edges, faces, and vertices.

Furthermore, we quantitatively define and describe the concept of DOCS for both 2D and 3D self-assembly. And thus, we are able to correlate the intrinsic relationship between stability and DOCS of assemblies, and directly compare the stability difference of 2D and 3D structures. The design and self-assembly strategy developed in this study as well as the potential applications will provide further insight into the current state of coordination-driven supramolecular chemistry, which has matured in the context of a large variety of macrocycles and polyhedra assembled by ditopic ligands.

RESULTS AND DISCUSSION

Synthesis, Self-Assembly and Characterization of Ring-in-Rings. Tetratopic ligand **1** was synthesized by several steps of Suzuki and Sonogashira couplings as shown in Scheme 2. Two alkyloxy chains were introduced to increase solubility of target assemblies and simplify ^{1}H NMR spectrum of aromatic region. The ^{1}H NMR spectrum of ligand **1** showed two sets of

Scheme 1. Self-Assemblies of Ring-in-Rings (R1 and R2) and Sphere-in-Sphere (S)

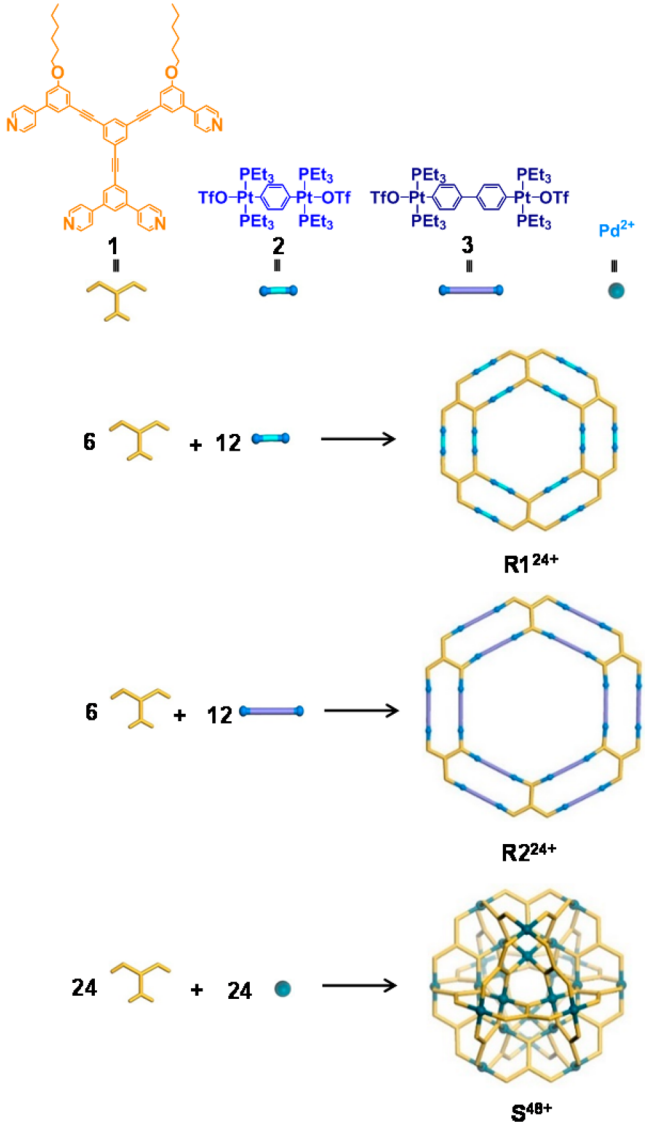

pyridine signals corresponding to the symmetric structure (Figure 1a). The assembled ring-in-rings (**R1** and **R2**) were achieved by mixing donor ligand **1** with the 180° diplatinum(II) acceptor **2** or **3**[18] in 1:2 ratio in DMSO-d_6, respectively for direct multinuclear NMR (^{1}H, ^{31}P, and ^{13}C) analysis and multidimensional mass spectrometry characterization.

^{1}H and ^{31}P NMR analysis of **R1** and **R2** revealed very similar characteristics, supporting the formation of discrete and highly symmetric architectures. As many previous study, the broad NMR signals were attributed to the tumbling motion of giant assemblies that were slow on the NMR time scale (Figure 1).[5d,f,19] In the ^{1}H NMR spectrum of each assembly, the α and β hydrogen atoms of the pyridine rings displayed down filed shifts (α-H, 0.23 ppm, β-H, 0.24 ppm) upon complexation of the pyridine-N atom with the Pt(II) center, indicating the loss of electron density (Figures 1a and S1a, Supporting Information).[20] Moreover, the single set signal of alkyloxy chains was another characteristic feature of discrete assembly and excluded the formation of oligomers. Further characterization by 2D NOESY was employed as well to facilitate ^{1}H NMR interpretation. Herein the presence of cross peaks

DOI: 10.1021/ja511443p
J. Am. Chem. Soc. 2015, 137, 1556−1564

Scheme 2. Synthesis of Ligand 1

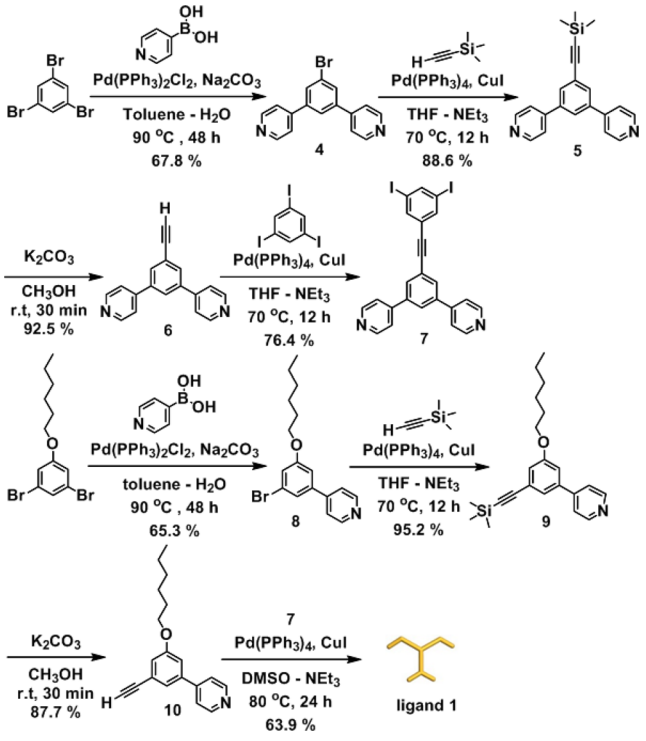

between the signals of the PEt_3 protons and the pyridine protons was observed (Figures S26 and S32), indicating that pyridyl groups are coordinated to Pt with phosphine ligands.

Because of the considerable broadening effect, ^{31}P NMR spectra of **R1** (Figure 1b) and **R2** (Figure S1b), which were shifted upfield (calculated 3.58 ppm for **R1** and 3.74 ppm for **R2**) from the starting diplatinum(II) acceptor **2** or **3**, only displayed one broad peak at 15.10 and 15.76 ppm, respectively. Theoretically, there should be two different signals for the inner and outer rims of ^{31}P. This also could be attributed to the quite similar chemical environment of ring-in-ring. Additionally the decrease in coupling of flanking ^{195}Pt satellites (ca. $\Delta J = -178.1$ Hz for **R1** and $\Delta J = -156.6$ Hz for **R2**) was observed. These changes are consistent with back-donation from the platinum atoms.[20] In diffusion-ordered NMR spectroscopy (DOSY) for **R1** (Figure 1c), the observation of a distinct band at log $D = -9.97$ suggested the formation of single product. Similarly, DOSY of **R2** showed one band at log $D = -10.02$, indicating a slightly larger size than **R1** (Figure S1c).

Multidimensional mass spectrometry including three levels of characterization, i.e., conventional electrospray ionization-mass spectrometry (ESI-MS), ion mobility-mass spectrometry (IM-MS)[21,22] and gradient tandem-mass spectrometry (gMS^2)[23] were employed to unambiguously address the molecular compositions, shapes, sizes and stability of these giant assemblies. In ESI-MS, a series of peaks with continuous charge states corresponding to losing different numbers of $CF_3SO_3^-$ counterions were detected along with negligible fragments (Figures 2a and S2a). The experimental isotope pattern of each charge state agreed well with theoretical simulations (Figures S5 and S6). After deconvolution, **R1** and **R2** were measured as 20 153 and 21 065 Da, respectively with molecular composition of 6 ligand **1** and 12 diplatinum(II) acceptor **2** or **3**. It is worth nothing that ESI-MS of many previous hexagon assembled by ditopic pyridyl-based ligands

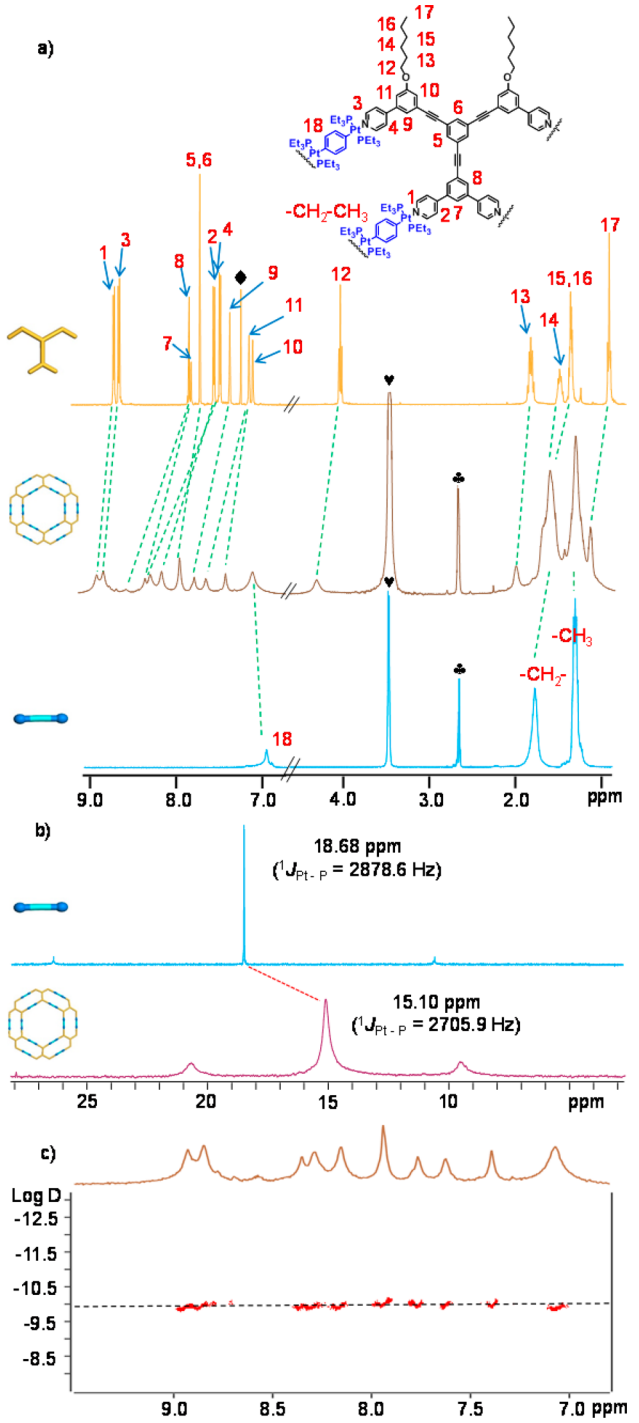

Figure 1. (a) ^1H NMR spectra of **1** (500 MHz, $CDCl_3$, 300 K), **R1** (500 MHz, DMSO-d_6, 330 K) and 180° diplatinum(II) acceptor **2**. Diamonds, hearts and clubs are signals for $CDCl_3$, DMSO-d_6 and D_2O respectively. (b) ^{31}P NMR (242.9 MHz, DMSO-d_6, 330 K) spectra of **R1** and 180° diplatinum(II) acceptor **2**. (c) 2D DOSY (500 MHz, DMSO-d_6, 330 K) spectrum of **R1**.

always produced vast fragments, which became a major obstacle to effective spectra interpretation and structural characterization.[20a,b] Therefore, these ring-in-rings with high DOCS significantly increased the stability of assemblies and thus facilitated mass spectrometry characterization.

As a powerful tool for macromolecular structure characterization, IM-MS was applied as the second level mass

DOI: 10.1021/ja511443p
J. Am. Chem. Soc. 2015, 137, 1556−1564

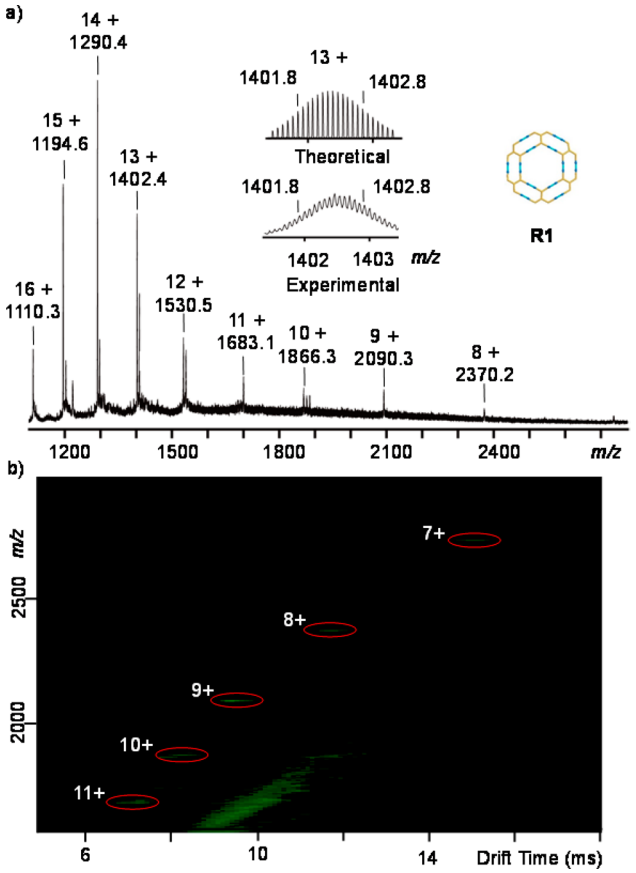

Figure 2. (a) ESI-MS of **R1**, with an inset showing the theoretical and experimental isotopic patterns of the 13^+ signal. (b) 2D ESI-IM-MS plot (m/z vs drift time) of **R1**. The charge states of intact assemblies are marked.

spectrometry analysis to address whether structural isomers or conformers existed (Figures 2b and S2b). IM-MS displayed signal of each charge state (7^+ to 11^+) with a narrow distribution as expected owing to the great rigidity and geometric constraints, indicating that there was no isomers or conformers. gMS^2 was applied as third level of mass spectrometry to evaluate the stability difference of supramolecular structures, particularly 2D vs 3D (vide infra). 15^+ charged ions of **R1** and **R2** were isolated by quadrupole for the following collision induced dissociation (CID), in which collision energy was gradually increased by changing the voltage of trap cell. Both **R1** and **R2** exhibited similar but low stability and completely dissociated at 8 and 10 V, corresponding to a same center-of-mass collision energy of 0.02, respectively (Figures 3 and S3).

To obtain more structural evidence, transmission electron microscopy (TEM) measurement was performed to directly visualize the sizes and shapes of these giant 2D architectures (Figures 4 and S4a, S4b). Both **R1** and **R2** with 24 Pt(II) ions bearing a high electron density significantly enhanced the contrast between two rims and central hollow region. In Figure 4, several nearly circular structures of **R1** are shown on carbon-coated copper grids with comparable size as theoretical diameter of 7.2 nm by modeling. As additional evidence, the images from AFM showed the morphology of the **R1** and **R2** as dots on the mica surface (Figure S4 and S35).

Self-Assembly and Characterization of Sphere-in-Sphere. As mentioned earlier, switching from terpyridine to

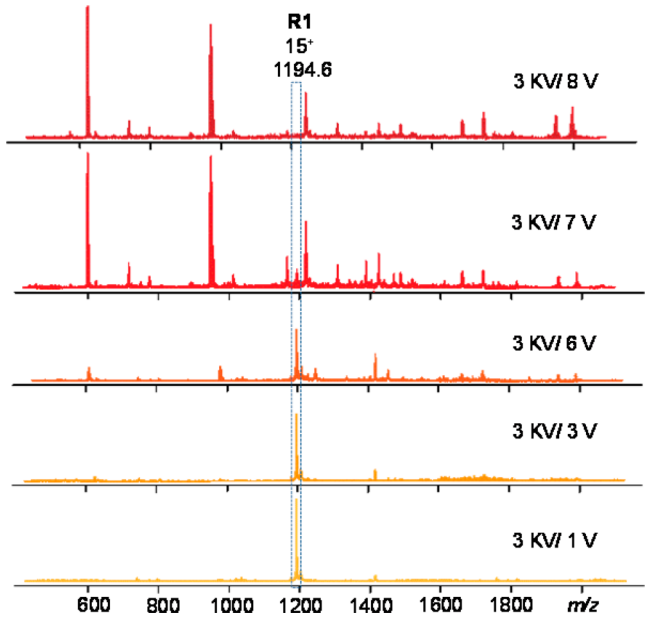

Figure 3. Gradient tandem-mass spectrometry (gMS^2) of **R1** at m/z 1194.6 (15^+) with different collision energy.

pyridyl-based self-assembly allowed us to step in more diverse 3D self-assembly. Accordingly, using naked Pd(II) ions instead of end-capped diplatinum(II) components, the self-assembly should form a sphere-in-sphere (**S**) structure consisting of 24 ligand **1** and 24 Pd(II) based on the elegant 3D $[M_nL_{2n}]$ assemblies reported by Fujita and co-workers.[5c,d,24] The stability of our target sphere-in-sphere with 96 coordination sites was expected to be improved considerably compared to the 24 coordination sites of ring-in-rings. Indeed, Fujita et al. reported a giant sphere-in-sphere with a flexible triethylene glycol linker connecting two spheres.[5e] If we assumed the design and self-assembly of Fujita's case was based on the exquisite arrangement of the inner and outer donor groups, our self-assembly with all rigid backbone emphasized the structural integrity and required precise preorganization of entire architecture (see the video of modeling structure in Supporting Information). The entire structure is not one continuous piece but is divided into many void spaces. Such sophisticated 3D structures with multiple subunits are reminiscent to protein tertiary structures, which contain different functional domains.

Self-assembly of **S** was performed by treating ligand **1** with an equimolar amount of $Pd(NO_3)_2$ in DMSO-d_6 at 80 °C for 12 h for direct NMR characterization (Figure 5). All the α and β hydrogen atoms of the pyridine rings shifted downfield (α-H, 0.97 and 0.84 ppm; β-H, 1.23 and 0.83 ppm) as a result of complexation of the pyridine-N atom with the Pd (II) center. Alkyloxy chains displayed single set of signals indicating the formation of a discrete product. Again, broad signals were observed in the ^{1}H NMR spectrum, suggesting the existence of a large assembly with slow tumbling motions.[5d,f,19] DOSY spectrum showed a single band at log $D = -9.96$, confirmed the formation of discrete product.

Multidimensional mass spectrometry provided more structural evidence supporting the proposed sphere-in-sphere. In Figure 6, a series of peaks with continuous charge states from 12^+ to 23^+ were detected in ESI-MS; however, we were not able to obtain high resolution isotopic distribution for each charge state. This was attributable to the high molecular weight

DOI: 10.1021/ja511443p
J. Am. Chem. Soc. 2015, 137, 1556−1564

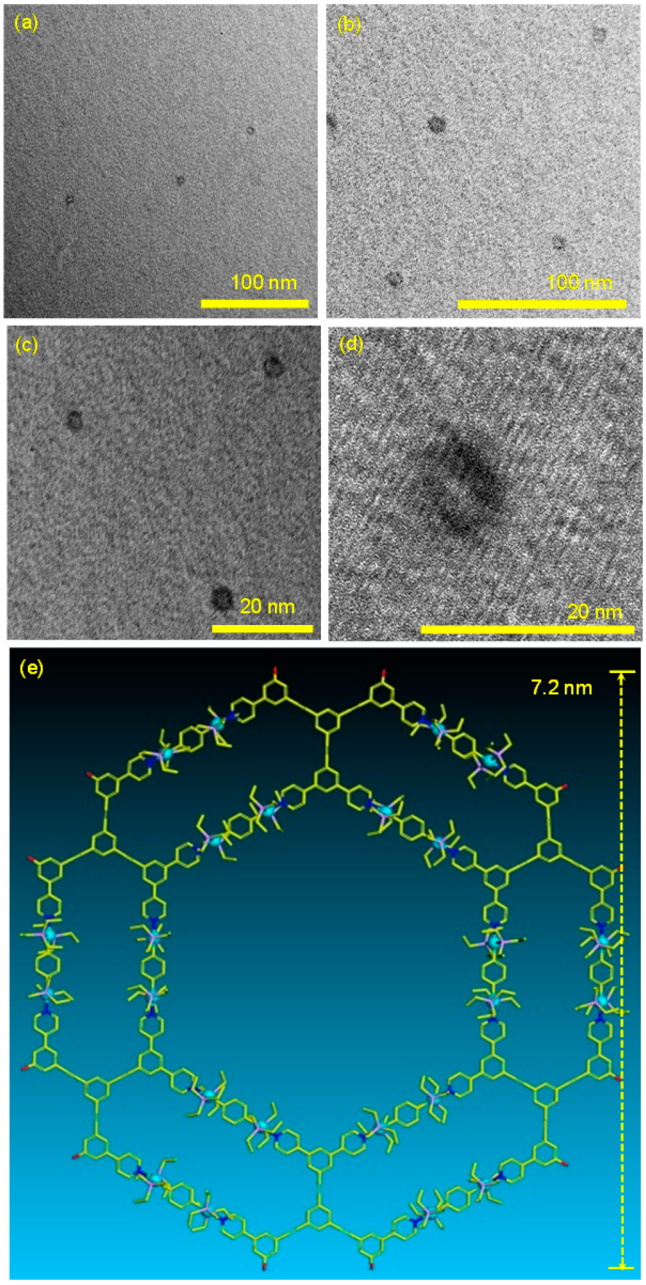

Figure 4. (a,b,c,d) TEM images of **R1** in different scale. (e) Representative energy-minimized structures from molecular modeling of **R1**. The alkyl chains are omitted for clarity in the molecular modeling.

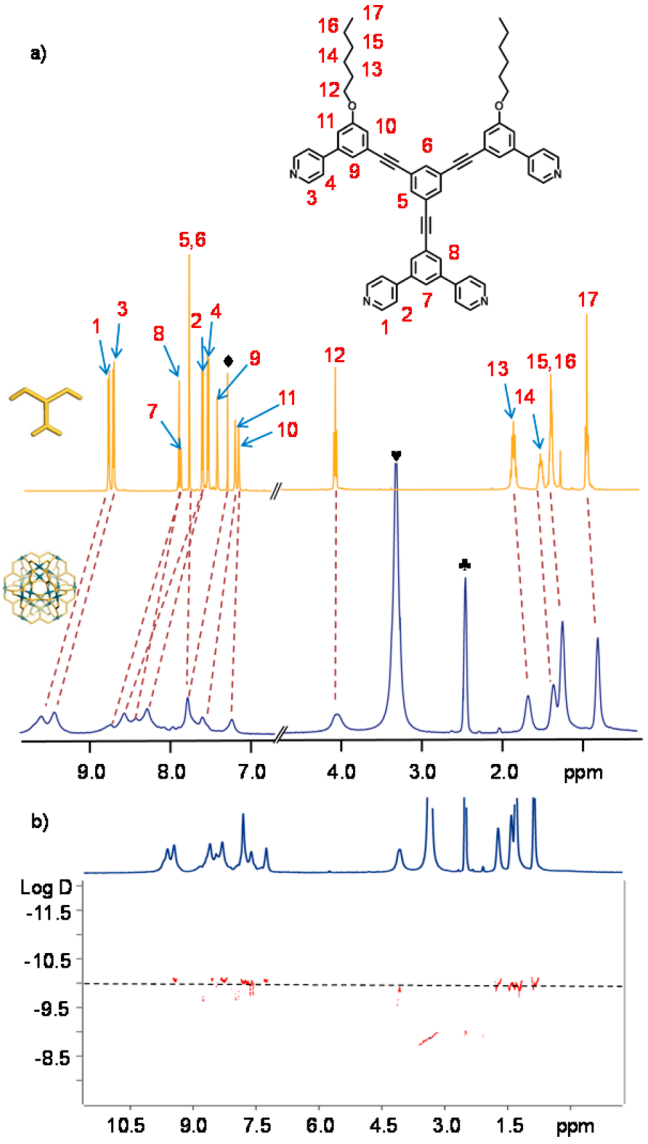

Figure 5. (a) ^{1}H NMR spectra of ligand **1** (500 MHz, $CDCl_3$, 300 K) and **S** with NO_3^- as counterion (500 MHz, DMSO-d_6, 330 K). Diamonds, hearts and clubs are signals for $CDCl_3$, DMSO-d_6 and D_2O respectively. (b) 2D DOSY (500 MHz, DMSO-d_6, 330 K) spectrum of **S**.

(theoretical molecular weight, 27991 Da), resolution limits of our instrument as well as the encapsulation of unknown numbers of solvent molecules in the large cavity. After deconvolution of m/z, the measured mass of **S** was calculated with average of 27992 Da, matched well with the formula of $[Pd_{24}(C_{64}H_{54}N_4O_2)_{24}]^{48+}\cdot 48(BF_4^-)$.

gMS^2 revealed the exceptional stability of **S** at collision energies ranging from 5 to 38 V (Figure 7). When the collision cell reached 38 V, which is significantly higher than 8 V of **R1** and 10 V of **R2**, the 15^+ ions (m/z 1779.1) completely disappeared, corresponding to a center-of-mass collision energy 0.06 eV. Because of the higher DOCS of sphere-in-sphere, it exhibited considerably higher stability than ring-in-rings.

All attempts to grow X-ray-quality single crystals of **S** have so far proven unsuccessful. Therefore, we carried out TEM and AFM measurements to visualize this sphere-in-sphere. TEM images (Figure 8) of the dried samples revealed particles with a weak contrast embedded in the thin film formed by the dried solvent. The measured size was comparable to the theoretical diameter of 5.8 nm from molecular modeling.

AFM imaging (Figure 9) was performed by dropping very dilute solution on freshly cleaved mica surface. We chose ten different areas (1000 nm × 1000 nm) and collected 129 dots to reach more accurate measured height with an average value of 5.5 nm, which is slightly smaller than the diameter of nanosphere by modeling (Figure 9g). We reasoned that these spheres laid on the mica substrate by one of the windows instead of the diameter orientation. Because of the unavoidable tip broadening effect,[25] the measured widths of the dots are much larger than that by TEM and the theoretical predicated diameter. Therefore, the measured heights by AFM are used to

DOI: 10.1021/ja511443p
J. Am. Chem. Soc. 2015, 137, 1556−1564

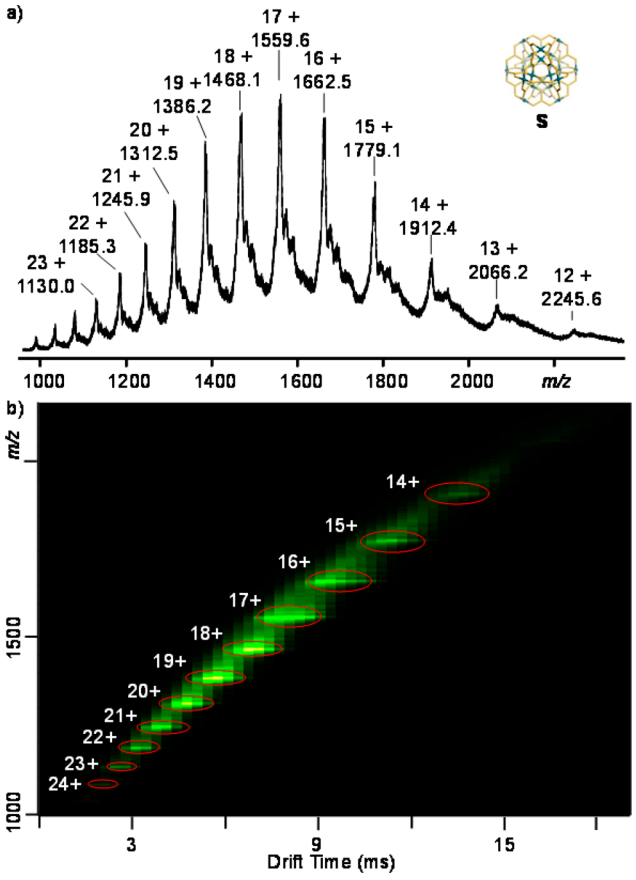

Figure 6. (a) ESI-MS and 2D ESI-IM-MS plot (m/z vs drift time) of **S** with BF_4^- as counterion. (b) The charge states of intact assemblies are marked.

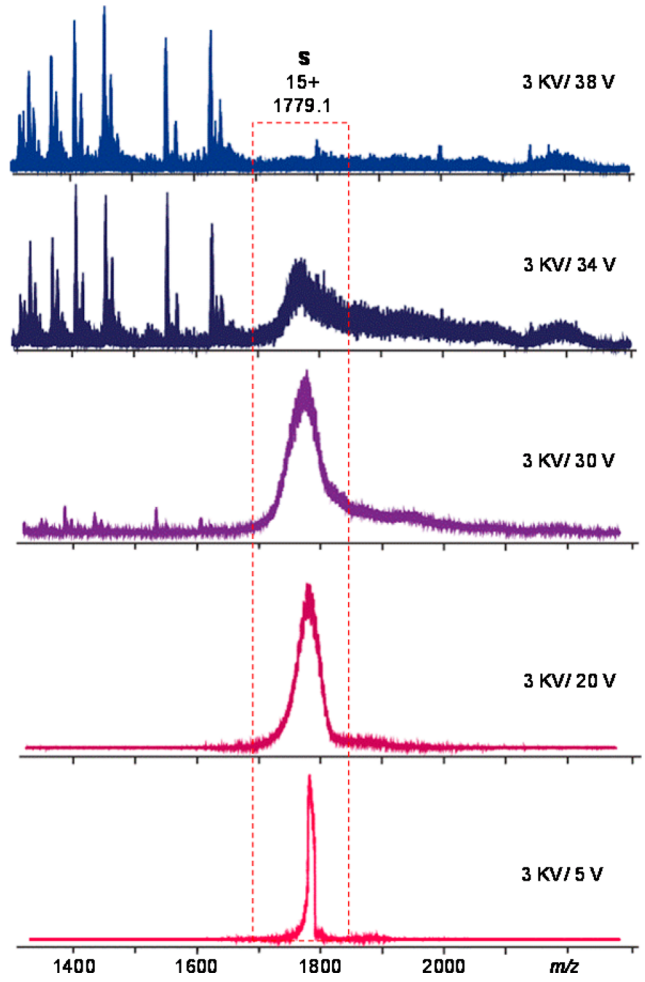

Figure 7. Gradient tandem-mass spectrometry (gMS^2) of **S** at m/z 1779.1 (15^+) with different collision energy.

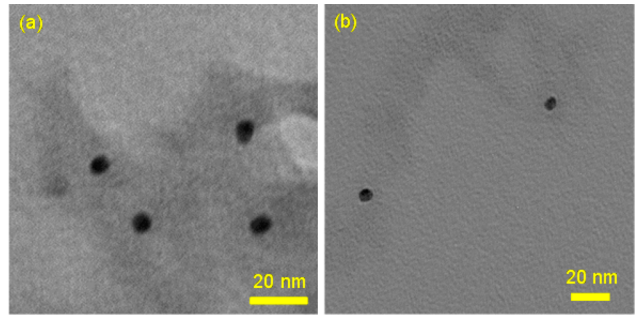

Figure 8. (a,b) TEM images of **S** with BF_4^- as counterion.

determine the diameter. With the high resolution amplitude image, we were able to visualize small dots on the supramolecular surface like a golf ball with an unsmooth surface, perhaps due to the alkyloxy chains on the outer shell. The entire outer layer is not one continuous piece but is divided into 12 domains surrounding the inner cage.

Comparison of the Stability of 2D and 3D Assemblies. Regarding the distinct stability between ring-in-ring and sphere-in-sphere, we reason that the origin of stability difference in these structures is the redundancy of the rings. In gMS^2, if one metal−ligand bond breaks in either inner or outer ring, the entire structure should not fall apart. Instead, both the inner and outer ring must be broken simultaneously. Note that if only large ring is counted, both ring-in-rings should possess two closed loops; while there should be eight closed loops in sphere-in-sphere. Therefore, sphere-in-sphere exhibited higher stability than ring-in-rings since multiple metal−ligand bonds might be broken but without destroying the structure in gMS_2.

Furthermore, we used the following formula to quantitatively define and evaluate DOCS of different 2D and 3D architectures and interpret the stability difference, i.e., center-of-mass collision energy obtained from gMS^2. Compared to the number of closed ring, DOCS also considers the size of structure.

$$\text{DOCS} = \frac{\text{total coordination sites}}{\text{theoretical collision cross section}}$$

The theoretical collision cross sections were calculated from 100 energy-minimized structures using trajectory method by MOBCAL as 2870, 3220, 4010 $Å^2$ for **R1**, **R2** and **S**, respectively.[26] Both **R1** and **R2** have 24 coordination sites, while **S** has 96 coordination sites. On the basis of this formula, the DOCS for **R1**, **R2** and **S** are 0.008, 0.007, and 0.024 site/$Å^2$, respectively. Since the DOCS of **S** is 3-fold of ring-in-rings' DOCS, there is no doubt about the enhanced stability of sphere-in-sphere as demonstrated in gMS^2. More interestingly, the center-of-mass collision energy of **S** is 0.06 eV, which is exactly three times as high as that of **R1** and **R2** at 0.02 eV. Therefore, we are able to correlate the relationship between DOCS and stability of assemblies in a quantitative manner. It is worth noting that DOCS is a very premature concept and is mainly introduced to specifically interpret gMS^2 data instead of guiding metallo-supramolecular design.

DOI: 10.1021/ja511443p
J. Am. Chem. Soc. 2015, 137, 1556−1564

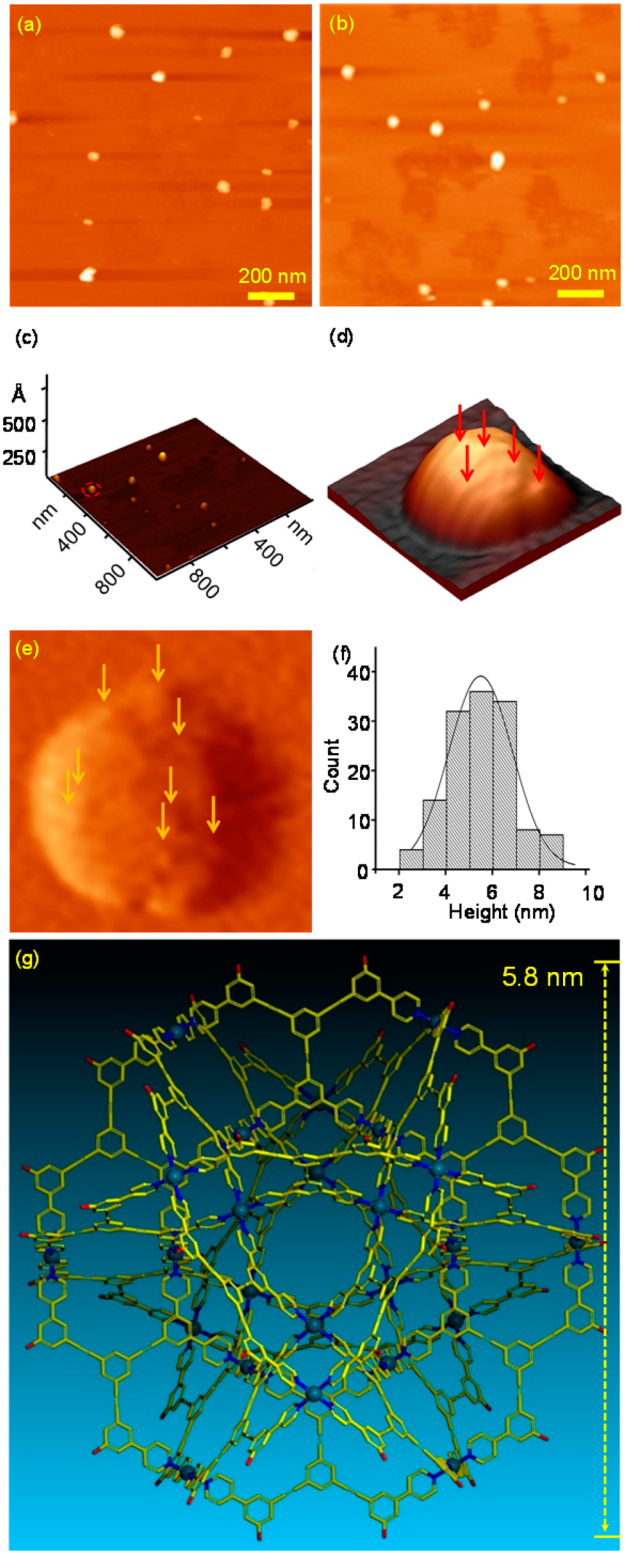

Figure 9. (a,b) AFM images of **S** with BF_4^- as counterion. (c) 3D AFM image. (d) Zoom-in 3D image of the dot labeled by red circle. (e) Amplitude individual 3D AFM image of the dot labeled by red circle. (f) Statistical height histogram of AFM for 129 dots. (g) Representative energy-minimized structure of **S** from molecular modeling. The long alkyl chains are omitted for clarity in the molecular modeling.

Supramolecular Gels Formed by R1 and R2. Interestingly, the self-assembled hexagons **R1** and **R2** could form organometallic temperature-responsive gels in some polar solvents. The formed supramolecular gels gradually turned into solutions upon heating, and subsequently reformed gels as the solutions were cooled down to room temperature. The critical gelator concentrations (CGCs) and gel-to-solution phase-transition temperature (T_{gel}) values of the complexes **R1** and **R2** in several different solvent systems were determined and given in Table S1 and S2. The morphologies of the xerogels, **R1** and **R2**, were examined by both scanning electron microscopy (SEM) and TEM. Three-dimensional (3D) networks comprised of entangled fibers that were responsible for the observed gelations were observed in SEM investigation for **R1** and **R2** in different solvents (Figures 10 and S41−S44).

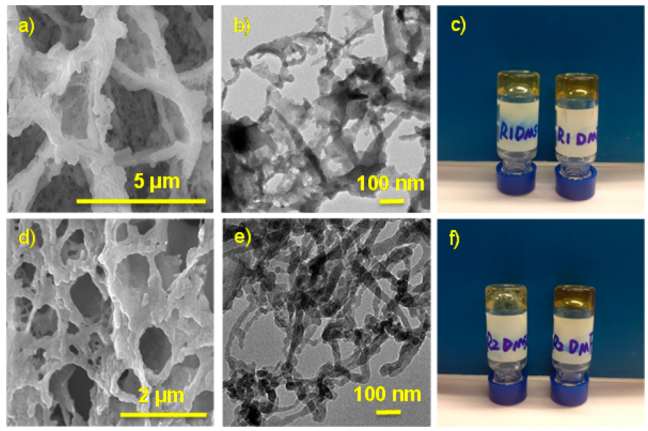

Figure 10. (a,d) SEM images of **R1** and **R2** xerogels in DMSO. (b,e) TEM images of **R1** and **R2** xerogels in DMSO. (c) Photograph of **R1** gel formation in DMSO (left) and DMF (right) at its CGCs. (f) Photograph of **R2** gel formation in DMSO (left) and DMF (right) at its CGCs.

The similar interconnected porous structures were found in TEM images, which were consistent with the discovery in SEM studies (Figure S45, S46). If the first level assembly is assumed as the spontaneous formation of multiple metal−ligand bonds to generate discrete cores, hierarchical self-assembly should be driven by dual intermolecular interactions, i.e., $\pi-\pi$ stacking and hydrophobic interactions in the second level to deliver complex materials. However, no gelation behavior was observed for sphere-in-sphere. It is worth to mention that supramolecular gels, particularly organometallic gels have played an important role in the development of soft material science,[27] and this design enriched the library of supramolecular metallogels herein.

CONCLUSIONS

Inspired by the cooperative multivalent interactions extensively utilized in biological systems, we have designed and assembled a series of 2D and 3D metallo-supramolecules through increasing the DOCS by one tetratopic pyridyl-based ligand with 180° diplatinum(II) acceptors and naked Pd(II), respectively. Compared to reported supramolecular hexagons and polyhedra by ditotpic ligands, the self-assembly of such giant architectures using multitopic ligands with all rigid backbone emphasized the structural integrity with precise preorganization of entire architecture, and required elaborate synthetic operations as well as extensive characterization. If we introduce different functionality at different subunits, this sophisticated 2D and 3D architectures may perform as proteins

DOI: 10.1021/ja511443p
J. Am. Chem. Soc. 2015, 137, 1556−1564

with different functional domains, which can never be achieved in regular 2D macrocycles or 3D polyhedrons. We reasoned that the number of closed rings was the origin of stability difference in these structures. We also proposed a quantitative definition for DOCS to compare between 2D and 3D metallo-supramolecular structures. With such definition, we were able to interpret the stability difference between 2D and 3D architectures obtained from gMS[2]. This concept can be expanded into other types of noncovalent interaction to evaluate stability. Moreover, the hierarchical self-assembly of 2D structures into the ordered nanostructures with gelation behavior will enrich the library of supramolecular metallogels and play an important role in the development of soft materials. Therefore, our future investigations are focused on design and self-assembly of giant supramolecular architectures with increasing complexity to enhance our design strategy guided by DOCS and explore the potential application, such as host–guest chemistry, template-directed synthesis and stimuli-responsive materials.

■ ASSOCIATED CONTENT

Supporting Information

Experimental procedures and characterization data. This material is available free of charge via the Internet at http://pubs.acs.org.

■ AUTHOR INFORMATION

Corresponding Authors

bxu@engr.uga.edu
hbyang@chem.ecnu.edu.cn
x_l8@txstate.edu

Author Contributions

[▽]B.S. and M.W. contributed equally.

Notes

The authors declare no competing financial interest.

■ ACKNOWLEDGMENTS

Xiaopeng Li acknowledges support of the National Science Foundation for PREM Center for Interfaces (DMR-1205670), NMR instrumentation (CHE-0946998), the Welch Foundation (AI-0045) and Research Enhancement Program of Texas State University. Hai-Bo Yang thanks the NSFC/China (No. 21132005 and 21322206) and the SMSTC (No. 13JC1402200) for financial support. Xiaohong Li thanks the NSFC/China (No. 21305098) and SRFDP (No. 20123201120014). Bin Sun acknowledges the visiting scholarship from East China Normal University. We gratefully acknowledge Dr. Luyi Sun and Jingjing Liu at University of Connecticut for TEM experiments.

■ REFERENCES

(1) (a) Cram, D. J. *Angew. Chem., Int. Ed. Engl.* **1988**, *27*, 1009. (b) Lehn, J.-M. *Angew. Chem., Int. Ed. Engl.* **1988**, *27*, 90. (c) Pedersen, C. J. *Angew. Chem., Int. Ed. Engl.* **1988**, *27*, 1021.

(2) (a) Lehn, J.-M. *Science* **2002**, *295*, 2400. (b) Lehn, J.-M. *Chem. Soc. Rev.* **2007**, *36*, 151. (c) Olenyuk, B.; Leininger, S.; Stang, P. J. *Chem. Rev.* **2000**, *100*, 853. (d) Davis, A. V.; Yeh, R. M.; Raymond, K. N. *Proc. Nat. Acad. Sci. U. S. A.* **2002**, *99*, 4793. (e) Hof, F.; Craig, S. L.; Nuckolls, C.; Rebek, J., Jr. *Angew. Chem., Int. Ed.* **2002**, *41*, 1488. (f) Rebek, J., Jr. *Acc. Chem. Res.* **2009**, *42*, 1660. (g) Forgan, R. S.; Sauvage, J.-P.; Stoddart, J. F. *Chem. Rev.* **2011**, *111*, 5434. (h) Holliday, B. J.; Mirkin, C. A. *Angew. Chem., Int. Ed.* **2001**, *40*, 2022. (i) Yoshizawa, M.; Klosterman, J. K.; Fujita, M. *Angew. Chem., Int. Ed.* **2009**, *48*, 3418. (j) Lagona, J.; Mukhopadhyay, P.; Chakrabarti, S.; Isaacs, L. *Angew. Chem., Int. Ed.* **2005**, *44*, 4844. (k) Hoeben, F. J. M.; Jonkheijm, P.; Meijer, E. W.; Schenning, A. P. H. J. *Chem. Rev.* **2005**, *105*, 1491. (l) Dalgarno, Scott J.; Jerry, N. P. P.; Atwood, L. *Coord. Chem. Rev.* **2008**, *252*, 825. (m) Niu, Z.; Gibson, H. W. *J. Am. Chem. Soc.* **2009**, *109*, 6024. (n) Hargrove, A. E.; Nieto, S.; Zhang, T.; Sessler, J. L.; Anslyn, E. V. *Chem. Rev.* **2011**, *111*, 6603. (o) Vukotica, V. N.; Loeb, S. J. *Chem. Soc. Rev.* **2012**, *41*, 5896.

(3) (a) Sauvage, J. P.; Collin, J. P.; Chambron, J. C.; Guillerez, S.; Coudret, C.; Balzani, V.; Barigelletti, F.; Cola, L. D.; Flamigni, L. *Chem. Rev.* **1994**, *94*, 993. (b) Seidel, S. R.; Stang, P. J. *Acc. Chem. Res.* **2002**, *35*, 972. (c) Würthner, F.; You, C.-C.; Saha-Möller, C. R. *Chem. Soc. Rev.* **2004**, *33*, 133. (d) Fujita, M.; Tominaga, M.; Hori, A.; Therrien, B. *Acc. Chem. Res.* **2005**, *38*, 369. (e) Lee, S. J.; Hupp, J. T. *Coord. Chem. Rev.* **2006**, *250*, 1710. (f) Lee, S. J.; Lin, W. *Acc. Chem. Res.* **2008**, *41*, 521. (g) Oliveri, C. G.; Ulmann, P. A.; Wiester, M. J.; Mirkin, C. A. *Acc. Chem. Res.* **2008**, *41*, 1618. (h) Saalfrank, R. W.; Maid, H.; Scheurer, A. *Angew. Chem., Int. Ed.* **2008**, *47*, 8794. (i) Pluth, M. D.; Bergman, R. G.; Raymond, K. N. *Acc. Chem. Res.* **2009**, *42*, 1650. (j) Northrop, B. H.; Zheng, Y.-R.; Chi, K.-W.; Stang, P. J. *Acc. Chem. Res.* **2009**, *42*, 1554. (k) Jina, P.; Dalgarno, S. J.; Atwood, J. L. *Coord. Chem. Rev.* **2010**, *254*, 1760. (l) Chakrabarty, R.; Mukherjee, P. S.; Stang, P. J. *Chem. Rev.* **2011**, *111*, 6810. (m) Smulders, M. M. J.; Riddell, I. A.; Browne, C.; Nitschke, J. R. *Chem. Soc. Rev.* **2013**, *42*, 1728. (n) Ward, M. D.; Raithby, P. R. *Chem. Soc. Rev.* **2013**, *42*, 1619. (o) Cook, T. R.; Zheng, Y.-R.; Stang, P. J. *Chem. Rev.* **2013**, *113*, 734. (p) Saha, M. L.; De, S.; Pramanika, S.; Schmittel, M. *Chem. Soc. Rev.* **2013**, *42*, 6860. (q) Ayme, J.-F.; Beves, J. E.; Campbella, C. J.; Leigh, D. A. *Chem. Soc. Rev.* **2013**, *42*, 1700. (r) Han, M.; Engelhard, D. M.; Clever, G. H. *Chem. Soc. Rev.* **2014**, *43*, 1848.

(4) (a) Olenyuk, B.; Levin, M. D.; Whiteford, J. A.; Shield, J. E.; Stang, P. J. *J. Am. Chem. Soc.* **1999**, *121*, 10434. (b) Olenyuk, B.; Whiteford, J. A.; Fechtenkotter, A.; Stang, P. J. *Nature* **1999**, *398*, 796. (c) Leininger, S.; Fan, J.; Schmitz, M.; Stang, P. J. *Proc. Nat. Acad. Sci. U. S. A.* **1999**, *97*, 1380. (d) Kuehl, C. J.; Kryschenko, Y. K.; Radhakrishnan, U.; Seidel, S. R.; Huang, S. D.; Stang, P. J. *Proc. Nat. Acad. Sci. U. S. A.* **2002**, *99*, 4932. (e) Kryschenko, Y. K.; Seidel, S. R.; Arif, A. M.; Stang, P. J. *J. Am. Chem. Soc.* **2003**, *125*, 5193. (f) Zheng, Y.-R.; Zhao, Z.; Wang, M.; Ghosh, K.; Pollock, J. B.; Cook, T. R.; Stang, P. J. *J. Am. Chem. Soc.* **2010**, *132*, 16873. (g) Wang, M.; Zheng, Y.-R.; Cook, T. R.; Stang, P. J. *Inorg. Chem.* **2011**, *50*, 6107. (h) Li, S.; Huang, J.; Zhou, F.; Cook, T. R.; Yan, X.; Ye, Y.; Zhu, B.; Zheng, B.; Stang, P. J. *J. Am. Chem. Soc.* **2014**, *136*, 5908. (i) Yan, X.; Xu, J.-F.; Cook, T. R.; Huang, F.; Yang, Q.-Z.; Tung, C.-H.; Stang, P. J. *Proc. Nat. Acad. Sci. U. S. A.* **2014**, *111*, 8717.

(5) (a) Fujita, M.; Oguro, D.; Miyazawa, M.; Oka, H.; Yamaguchi, K.; Ogura, K. *Nature* **1995**, *378*, 469. (b) Fujita, M.; Fujita, N.; Ogura, K.; Yamaguchi, K. *Nature* **1999**, *400*, 52. (c) Tominaga, M.; Suzuki, K.; Kawano, M.; Kusukawa, T.; Ozeki, T.; Sakamoto, S.; Yamaguchi, K.; Fujita, M. *Angew. Chem., Int. Ed.* **2004**, *43*, 5621. (d) Sun, Q.-F.; Iwasa, J.; Ogawa, D.; Ishido, Y.; Sato, S.; Ozeki, T.; Sei, Y.; Yamaguchi, K.; Fujita, M. *Science* **2010**, *328*, 1144. (e) Sun, Q.-F.; Murase, T.; Sato, S.; Fujita, M. *Angew. Chem., Int. Ed.* **2011**, *50*, 10318. (f) Sun, Q.-F.; Sato, S.; Fujita, M. *Nat. Chem.* **2012**, *4*, 330. (g) Harris, K.; Sun, Q.-F.; Sato, S.; Fujita, M. *J. Am. Chem. Soc.* **2013**, *135*, 12497. (h) Sawada, T.; Hisada, H.; Fujita, M. *J. Am. Chem. Soc.* **2014**, *136*, 4449.

(6) (a) Beissel, T.; Powers, R. E.; Raymond, K. N. *Angew. Chem., Int. Ed. Engl.* **1996**, *35*, 1084. (b) Caulder, D. L.; Brückner, C.; Powers, R. E.; König, S.; Parac, T. N.; Leary, J. A.; Raymond, K. N. *J. Am. Chem. Soc.* **2001**, *123*, 8923. (c) Zhao, C.; Sun, Q.-F.; Hart-Cooper, W. M.; DiPasquale, A. G.; Toste, F. D.; Bergman, R. G.; Raymond, K. N. *J. Am. Chem. Soc.* **2013**, *135*, 18802. (d) Wang, Z. J.; Clary, K. N.; Bergman, R. G.; Raymond, K. N.; Toste, F. D. *Nat. Chem.* **2013**, *5*, 100.

(7) (a) Mal, P.; Schultz, D.; Beyeh, K.; Rissanen, K.; Nitschke, J. R. *Angew. Chem., Int. Ed.* **2008**, *47*, 8297. (b) Mal, P.; Breiner, B.; Rissanen, K.; Nitschke, J. R. *Science* **2009**, *324*, 1697. (c) Riddell, I. A.; Smulders, M. M. J.; Clegg, J. K.; Hristova, Y. R.; Breiner, B.; Thoburn, J. D.; Nitschke, J. R. *Nat. Chem.* **2012**, *4*, 751. (d) Bilbeisi, R. A.;

DOI: 10.1021/ja511443p
J. Am. Chem. Soc. 2015, 137, 1556–1564

Ronson, T. K.; Nitschke, J. R. *Angew. Chem., Int. Ed. Engl.* **2013**, *52*, 9027. (e) Riddell, I. A.; Hristova, Y. R.; Clegg, J. K.; Wood, C. S.; Breiner, B.; Nitschke, J. R. *J. Am. Chem. Soc.* **2013**, *135*, 2723. (f) Meng, W.; League, A. B.; Ronson, T. K.; Clegg, J. K.; Isley, W. C.; Semrouni, D.; Gagliardi, L.; Cramer, C. J.; Nitschke, J. R. *J. Am. Chem. Soc.* **2014**, *136*, 3972. (g) Jiménez, A.; Bilbeisi, R. A.; Ronson, T. K.; Zarra, S.; Woodhead, C.; Nitschke, J. R. *Angew. Chem., Int. Ed.* **2014**, *53*, 4556.

(8) (a) Ayme, J.-F.; Beves, J. E.; Leigh, D. A.; McBurney, R. T.; Rissanen, K.; Schultz, D. *Nat. Chem.* **2011**, *4*, 15. (b) Ayme, J.-F.; Beves, J. E.; Leigh, D. A.; McBurney, R. T.; Rissanen, K.; Schultz, D. *J. Am. Chem. Soc.* **2012**, *134*, 9488. (c) Beves, J. E.; Campbell, C. J.; Leigh, D. A.; Pritchard, R. G. *Angew. Chem., Int. Ed.* **2013**, *52*, 6464.

(9) (a) Fowler, D. A.; Mossine, A. V.; Beavers, C. M.; Teat, S. J.; Dalgarno, S. J.; Atwood, J. L. *J. Am. Chem. Soc.* **2011**, *133*, 11069. (b) Fowler, D. A.; Rathnayake, A. S.; Kennedy, S.; Kumari, H.; Beavers, C. M.; Teat, S. J.; Atwood, J. L. *J. Am. Chem. Soc.* **2013**, *135*, 12184.

(10) (a) Hiraoka, S.; Harano, K.; Shiro, M.; Ozawa, Y.; Yasuda, N.; Toriumi, K.; Shionoya, M. *Angew. Chem., Int. Ed.* **2006**, *45*, 6488. (b) Hiraoka, S.; Harano, K.; Shiro, M.; Shionoya, M. *J. Am. Chem. Soc.* **2008**, *130*, 14368. (c) Hiraoka, S.; Yamauchi, Y.; Arakane, R.; Shionoya, M. *J. Am. Chem. Soc.* **2009**, *131*, 11646.

(11) (a) Clever, G. H.; Kawamura, W.; Tashiro, S.; Shiro, M.; Shionoya, M. *Angew. Chem., Int. Ed.* **2012**, *51*, 2606. (b) Engelhard, D. M.; Freye, S.; Grohe, K.; John, M.; Clever, G. H. *Angew. Chem., Int. Ed.* **2012**, *51*, 4747. (c) Frank, M.; Hey, J.; Balcioglu, I.; Chen, Y.-S.; Stalke, D.; Suenobu, T.; Fukuzumi, S.; Frauendorf, H.; Clever, G. H. *Angew. Chem., Int. Ed.* **2013**, *52*, 10102.

(12) (a) Li, J.-R.; Zhou, H.-C. *Nat. Chem.* **2010**, *2*, 893. (b) Li, J.-R.; Yakovenko, A. A.; Lu, W.; Timmons, D. J.; Zhuang, W.; Yuan, D.; Zhou, H.-C. *J. Am. Chem. Soc.* **2010**, *132*, 17599. (c) Park, J.; Sun, L.-B.; Chen, Y.-P.; Perry, Z.; Zhou, H.-C. *Angew. Chem., Int. Ed.* **2014**, *53*, 5842.

(13) (a) Mirtschin, S.; Slabon-Turski, A.; Scopelliti, R.; Velders, A. H.; Severin, K. *J. Am. Chem. Soc.* **2010**, *132*, 14004. (b) Granzhan, A.; Schouwey, C.; Riis-Johannessen, T.; Scopelliti, R.; Severin, K. *J. Am. Chem. Soc.* **2011**, *133*, 7106. (c) Stephenson, A.; Argent, S. P.; Riis-Johannessen, T.; Tidmarsh, I. S.; Ward, M. D. *J. Am. Chem. Soc.* **2011**, *133*, 858. (d) Mahata, K.; Frischmann, P. D.; Würthner, F. *J. Am. Chem. Soc.* **2013**, *135*, 15656. (e) Chepelin, O.; Ujma, J.; Barran, P. E.; Lusby, P. J. *Angew. Chem., Int. Ed.* **2012**, *51*, 4194. (f) Lusby, P. J.; Müller, P.; Pike, S. J.; Slawin, A. M. Z. *J. Am. Chem. Soc.* **2009**, *131*, 16398.

(14) Fasting, C.; Schalley, C. A.; Weber, M.; Seitz, O.; Hecht, S.; Koksch, B.; Dernedde, J.; Graf, C.; Knapp, E.-W.; Haag, R. *Angew. Chem., Int. Ed.* **2012**, *51*, 10472.

(15) Wang, M.; Wang, C.; Hao, X.-Q.; Liu, J.; Li, X.; Xu, C.; Lopez, A.; Sun, L.; Song, M.-P.; Yang, H.-B.; Li, X. *J. Am. Chem. Soc.* **2014**, *136*, 6664.

(16) (a) Schubert, U. S.; Eschbaumer, C. *Angew. Chem., Int. Ed.* **2002**, *41*, 2892. (b) Hofmeier, H.; Schubert, U. S. *Chem. Soc. Rev.* **2004**, *33*, 373. (c) Constable, E. C. *Chem. Soc. Rev.* **2007**, *36*, 246. (d) Constable, E. C. *Coord. Chem. Rev.* **2008**, *252*, 842. (e) Eryazici, I.; Moorefield, C. N.; Newkome, G. R. *Chem. Rev.* **2008**, *108*, 1834. (f) De, S.; Mahata, K.; Schmittel, M. *Chem. Soc. Rev.* **2010**, *39*, 1555. (g) Wild, A.; Winter, A.; Schlütter, F.; Schubert, U. S. *Chem. Soc. Rev.* **2011**, *40*, 1459. (h) Winter, A.; Hoeppener, S.; Newkome, G. R.; Schubert, U. S. *Adv. Mater.* **2011**, *23*, 3484.

(17) (a) Bassani, D. M.; Lehn, J.-M.; Fromm, K.; Fenske, D. *Angew. Chem., Int. Ed.* **1998**, *37*, 2364. (b) Barboiu, M.; Vaughan, G.; Graff, R.; Lehn, J.-M. *J. Am. Chem. Soc.* **2003**, *125*, 10257. (c) Chan, Y.-T.; Li, X.; Soler, M.; Wang, J.-L.; Wesdemiotis, C.; Newkome, G. R. *J. Am. Chem. Soc.* **2009**, *131*, 16395. (d) Mahata, K.; Schmittel, M. *J. Am. Chem. Soc.* **2009**, *131*, 16544. (e) Mahata, K.; Saha, M. L.; Schmittel, M. *J. Am. Chem. Soc.* **2010**, *132*, 15933. (f) Chan, Y.-T.; Li, X.; Yu, J.; Carri, G. A.; Moorefield, C. N.; Newkome, G. R.; Wesdemiotis, C. *J. Am. Chem. Soc.* **2011**, *133*, 11967. (g) Wang, J.-L.; Li, X.; Lu, X.; Hsieh, I.-F.; Cao, Y.; Moorefield, C. N.; Wesdemiotis, C.; Cheng, S. Z. D.; Newkome, G. R. *J. Am. Chem. Soc.* **2011**, *133*, 11450. (h) Schultz, A.; Li, X.; Barkakaty, B.; Moorefield, C. N.; Wesdemiotis, C.; Newkome, G. R. *J. Am. Chem. Soc.* **2012**, *134*, 7672. (i) Zheng, Z.; Opilik, L.; Schiffmann, F.; Liu, W.; Bergamini, G.; Ceroni, P.; Lee, L.-T.; Schütz, A.; Sakamoto, J.; Zenobi, R.; VandeVondele, J.; Schlüter, A. D. *J. Am. Chem. Soc.* **2014**, *136*, 6103. (j) Fermi, A.; Bergamini, G.; Roy, M.; Gingras, M.; Ceroni, P. *J. Am. Chem. Soc.* **2014**, *136*, 6395.

(18) (a) Manna, J.; Whiteford, J. A.; Stang, P. J.; Muddiman, D. C.; Smith, R. D. *J. Am. Chem. Soc.* **1996**, *118*, 8731. (b) Manna, J.; Kuehl, C. J.; Whiteford, J. A.; Stang, P. J. *Organometallics* **1997**, *16*, 1897.

(19) Black, S. P.; Stefankiewicz, A. R.; Smulders, M. M. J.; Sattler, D.; Schalley, C. A.; Nitschke, J. R.; Sanders, J. K. M. *Angew. Chem., Int. Ed.* **2013**, *52*, 5749.

(20) (a) Yang, H.-B.; Hawkridge, A. M.; Huang, S. D.; Das, N.; Bunge, S. D.; Muddiman, D. C.; Stang, P. J. *J. Org. Chem.* **2007**, *129*, 2120. (b) Yang, H.-B.; Ghosh, K.; Zhao, Y.; Northrop, B. H.; Lyndon, M. M.; Muddiman, D. C.; White, H. S.; Stang, P. J. *J. Am. Chem. Soc.* **2008**, *130*, 839. (c) Ghosh, K.; Yang, H.-B.; Northrop, B. H.; Lyndon, M. M.; Zheng, Y.-R.; Muddiman, D. C.; Stang, P. J. *J. Am. Chem. Soc.* **2008**, *130*, 5320.

(21) (a) Bowers, M. T.; Kemper, P. R.; von Helden, G.; van Koppen, P. A. M. *Science* **1993**, *260*, 1446. (b) Hoaglund-Hyzer, C. S.; Counterman, A. E.; Clemmer, D. E. *Chem. Rev.* **1999**, *99*, 3037. (c) Trimpin, S.; Plasencia, M.; Isailovic, D.; Clemmer, D. E. *Anal. Chem.* **2007**, *79*, 7965. (d) Bernstein, S. L.; Dupuis, N. F.; Lazo, N. D.; Wyttenbach, T.; Condron, M. M.; Bitan, G.; Teplow, D. B.; Shea, J.-E.; Ruotolo, B. T.; Robinson, C. V.; Bowers, M. T. *Nat. Chem.* **2009**, *1*, 326. (e) Silveira, J. A.; Fort, K. L.; Kim, D.; Servage, K. A.; Pierson, N. A.; Clemmer, D. E.; Russell, D. H. *J. Am. Chem. Soc.* **2013**, *135*, 19147.

(22) (a) Ruotolo, B. T.; Giles, K.; Campuzano, I.; Sandercock, A. M.; Bateman, R. H.; Robinson, C. V. *Science* **2005**, *310*, 1658. (b) Ruotolo, B. T.; Benesch, J. L. P.; Sandercock, A. M.; Hyung, S.-J.; Robinson, C. V. *Nat. Protoc.* **2008**, *3*, 1139. (c) Scarff, C. A.; Snelling, J. R.; Knust, M. M.; Wilkins, C. L.; Scrivens, J. H. *J. Am. Chem. Soc.* **2012**, *134*, 9193. (d) Thiel, J.; Yang, D.; Rosnes, M. H.; Liu, X.; Yvon, C.; Kelly, S. E.; Song, Y.-F.; Long, D.-L.; Cronin, L. *Angew. Chem., Int. Ed.* **2011**, *123*, 9033. (e) Ujma, J.; Cecco, M. D.; Chepelin, O.; Levene, H.; Moffat, C.; Pike, S. J.; Lusby, P. J.; Barran, P. E. *Chem. Commun.* **2012**, *48*, 4423.

(23) (a) Li, X.; Chan, Y.-T.; Wesdemiotis, C.; Newkome, G. R. *Anal. Chem.* **2011**, *83*, 1284. (b) Perera, S.; Li, X.; Soler, M.; Wesdemiotis, C.; Moorefield, C. N.; Newkome, G. R. *Angew. Chem., Int. Ed.* **2010**, *49*, 6539.

(24) Bunzen, J.; Iwasa, J.; Bonakdarzadeh, P.; Numata, E.; Rissanen, K.; Sato, S.; Fujita, M. *Angew. Chem., Int. Ed.* **2012**, *51*, 3161.

(25) (a) Radmacher, M.; Fritz, M.; Hansma, H.; Hansma, P. *Science* **1994**, *265*, 1577. (b) Chen, G.; Zhou, J.; Park, B.; Xu, B. *Appl. Phys. Lett.* **2009**, *95*, 043103. (c) Ichijo, T.; Sato, S.; Fujita, M. *J. Am. Chem. Soc.* **2013**, *135*, 6786.

(26) (a) Shvartsburg, A. A.; Jarrold, M. F. *Chem. Phys. Lett.* **1996**, *261*, 86. (b) Shvartsburg, A. A.; Liu, B.; Siu, K. W. M.; Ho, K. M. *J. Phys. Chem. A* **2000**, *104*, 6152.

(27) (a) Piepenbrock, M.-O. M.; Lloyd, G. O.; Clarke, N.; Steed, J. W. *Chem. Rev.* **2011**, *110*, 1960. (b) Tam, A. Y.-Y.; Yam, V. W.-W. *Chem. Soc. Rev.* **2013**, *42*, 1540.

DOI: 10.1021/ja511443p
J. Am. Chem. Soc. 2015, 137, 1556−1564